

PHASE SPACE ACCEPTANCE OF LMF TRANSPORT SCHEMES*

C. L. Olson
Sandia National Laboratories
Albuquerque, New Mexico 87185

Abstract

Three different ion beam transport schemes (achromatic lens, wire-guided transport, Z-discharge channel) for the light ion beam driver for the Laboratory Microfusion Facility (LMF) are examined analytically. For each case the phase space acceptance area is investigated, including the effects of angular momentum.

Introduction

Transport and focus of intense, voltage-ramped, ion beams over distances of several meters is required for the light ion beam driver for the Laboratory Microfusion Facility (LMF).¹ The baseline case^{2,3} is achromatic and uses ballistic transport at large radius from the diode (outer radius R) to a solenoidal lens, and then ballistic drift down to the target of radius r_p (Fig. 1). The back-up cases use wire-guided transport (Fig. 2) or Z-discharge channel transport (Fig. 3) with ballistic focus from the diode down to a small radius r_c ($< r_p$), transport in the channel at radius r_c , and then a short (few cm) ballistic drift to the target. Here we will examine the phase space acceptance area of each case, including the effects of angular momentum.

Ballistic Drift/Solenoidal Lens

The ballistic drift/solenoidal lens transport scheme is shown in Fig. 1.^{2,3} The beam is transported ballistically through a charge and current neutralized region, at essentially constant radius, from the diode to the lens. On exiting the lens, every particle trajectory may be characterized by its three parameters r_0 , $\theta_0 \equiv v_{r0}/v_z$, and $\phi_0 \equiv v_{\phi 0}/v_z$ where the three velocity components are v_r , v_ϕ , v_z . For acceptance, the trajectory must reach the target with $0 \leq r_1 \leq r_p$. The only restriction on ϕ_0 acceptance is to have

$$\phi_0 L \leq r_p, \quad (1)$$

which is simply a statement that the beam microdivergence θ_μ at the lens must have $\theta_\mu L \leq r_p$. For LMF parameters with $L = 150$ cm and $r_p = 1.0$ cm, this restricts ϕ_0 to

$$\phi_0 \leq 6.7 \text{ mrad}. \quad (2)$$

The simple acceptance criterion (2) does not depend on r_0 . For the following wire-guided and Z-discharge channel cases, we will find more complicated restrictions on ϕ_0 .

Wire-Guided Transport

The wire-guided transport scheme is shown schematically in Fig. 2. The beam leaves the diode and drifts ballistically, in a charge and current neutralized region, up to the entrance to the wire region. The wire radius is r_w , the confined beam radius is r_c , and the wire current is established before the beam arrives. The beam enters the wire region (which is also charge and current neutralized) at radius r_1 . For given initial parameters (r_0 , θ_0) we wish to determine the range of ϕ_0 values that will result in trapped ion trajectories confined to the range $r_w \leq r_1 \leq r_c$.

The three components of the ion equation of motion in the wire region are

$$M\dot{v}_r = -(q/c)v_z B_\phi + Mv_\phi^2/r, \quad (3a)$$

$$M\dot{v}_\phi = -Mv_r v_\phi/r, \quad (3b)$$

$$M\dot{v}_z = (q/c)v_r B_\phi, \quad (3c)$$

where M is the ion mass, q is the ion charge, and c is the speed of light. The wire magnetic field B_ϕ is

$$B_\phi = B_0(r_c/r) \quad r_w \leq r \leq r_c. \quad (4)$$

Equation (3b) integrates to give

$$rv_\phi = \text{const}, \quad (5)$$

which just expresses conservation of angular momentum. From Eq. (3c) we may assume $v_z \approx \text{const}$ provided

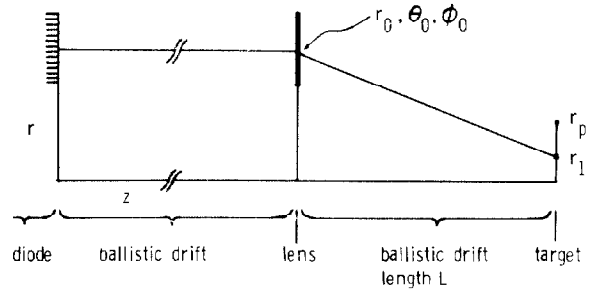


Figure 1. Ballistic transport/solenoid lens.

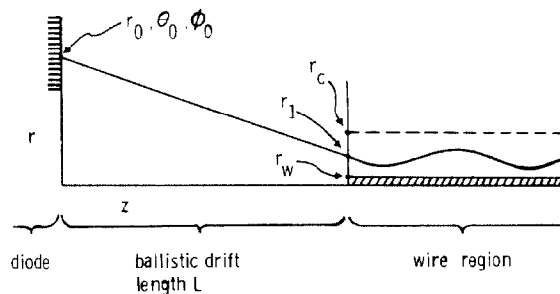


Figure 2. Wire-guided transport.

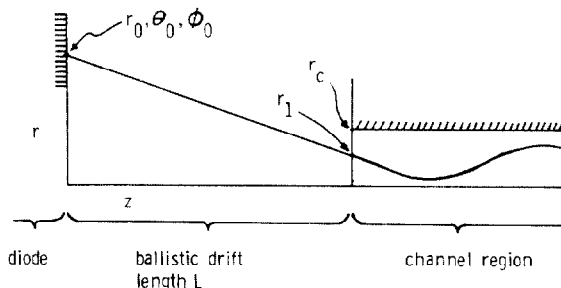


Figure 3. Channel transport.

*This work was supported by the U.S. Department of Energy under Contract DE-AC04-76DP00789.

$$v_r/v_z \ll [Mc/(qB_\phi)]/t_1, \quad (6)$$

which is typically satisfied. (Here t_1 is the ion transit time.) Using these results in Eq. (3a), we find

$$\ddot{r} = -(qv_z B_\phi r_c)/(Mc)(1/r) + [r_0^2 v_\phi^2]/r^3. \quad (7)$$

Setting $\ddot{r} = 0$ gives for the equilibrium radius

$$r_{eq} = r_0 \phi_0 [(\beta Mc^2/q)/(B_\phi r_c)]^{1/2}, \quad (8)$$

where $\beta = v_z/c$. Alternatively, if the particle enters the wire region at radius r_1 , it will stay at that radius provided $\theta_0 = 0$, and provided

$$\phi_0 = (r_1/r_0)[(\beta Mc^2/q)/(B_\phi r_c)]^{1/2}. \quad (9)$$

The trajectory trapping constraints may now be found as follows. Multiplying Eq. (9) by idt and integrating, we find that at an extremum of the trajectory ($r = r_{max}$ or $r = r_{min}$),

$$\theta_0^2 = 4(I_w/I_A) \ln(r/r_1) + (r_0^2 v_\phi^2/v_z^2)(r^2 - r_1^2), \quad (10)$$

where I_w is the wire current and $I_A = \beta \gamma Mc^3/q$ is the ion Alfvén current. Substituting $r = r_c$ or $r = r_w$ into Eq. (10), we obtain the constraints on ϕ_0 as

$$\phi_0^2 = \frac{4(I_w/I_A) \ln(r_c/r_1) - \theta_0^2}{(r_0^2/r_c^2)[(r_c^2/r_1^2) - 1]} \quad r_1 \leq r_c, \quad (11)$$

$$\phi_0^2 = \frac{4(I_w/I_A) \ln(r_1/r_w) + \theta_0^2}{(r_0^2/r_w^2)[1 - (r_w^2/r_1^2)]} \quad r_1 \geq r_w. \quad (12)$$

These results are plotted in Figs. 4-6 for some typical LMF parameter values ($r_w = 0.05$ cm, $r_c = 0.7$ cm, $I_w = 50$ kA, $I_A = 7.0$ MA for 30 MeV Li^{+3}). In all cases, the upper (lower) boundary curve is given by Eq. (11) [Eq. (12)]. Figure 4 shows the

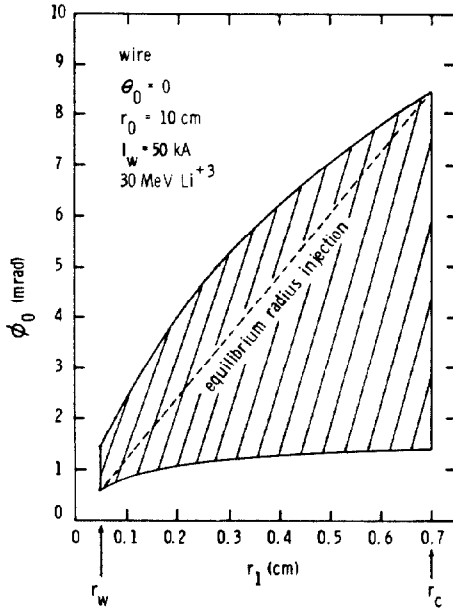


Figure 4. Wire acceptance region for $\theta_0 = 0$ and $r_0 = 10$ cm.

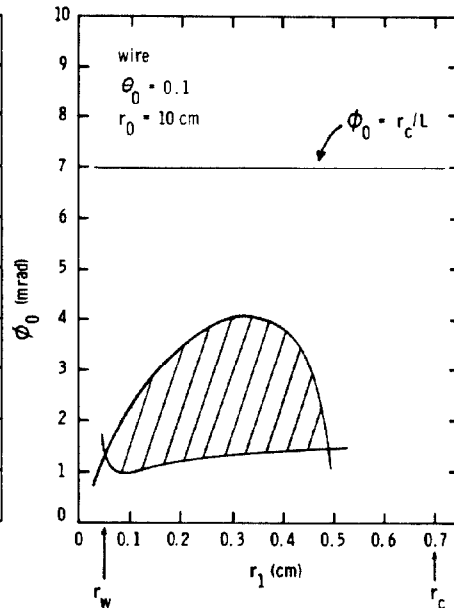


Figure 5. Wire acceptance region for $\theta_0 = 0.1$ and $r_0 = 10$ cm.

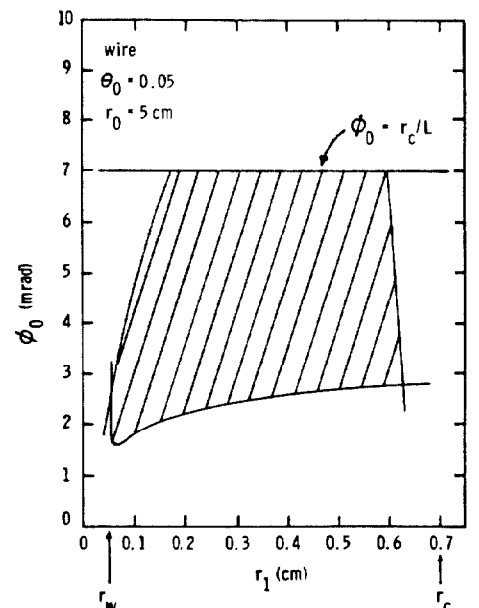


Figure 6. Wire acceptance region for $\theta_0 = 0.05$ and $r_0 = 5$ cm.

acceptance region for the hypothetical case $\theta_0 = 0$. The equilibrium radius injection condition given by Eq. (9) is also shown. Note that a small amount of angular momentum is needed to miss hitting the wire, but only slightly more angular momentum makes the beam too difficult to contain within radius r_c . Actually, Fig. 4 represents a necessary, but not sufficient, condition for trapping since the constraint

$$\phi_0 L \leq r_c, \quad (13)$$

must also be satisfied. Figures 5 and 6 represent cases that satisfy (13) for an LMF diode with an outer radius $r_0 = 10$ cm, an inner radius $r_0 = 5$ cm, and a length $L = 100$ cm. Figure 5 (Fig. 6) corresponds to ions emitted at the outer radius (inner radius) of the diode. Note that careful phase space tailoring of the beam is required to insure that most of the beam will be in the acceptance regions.

Z-Discharge Channel Transport

The Z-discharge channel transport scheme is shown schematically in Fig. 3. The diode and ballistic drift regions are the same as for the wire transport case. However, in the channel region, a pre-formed Z-discharge exists with

$$B_\phi = B_0(r/r_c) \quad 0 \leq r \leq r_c. \quad (14)$$

There is no obstruction on axis (as in the wire case) and ions may freely pass through $r = 0$. Combining Eqs. (3a), (5), and (14), we find for the radial equation of motion

$$\ddot{r} = -(qv_z B_0)/(Mcr_c)]r + (r_0^2 v_\phi^2)/r^3. \quad (15)$$

Setting $\ddot{r} = 0$ gives for the equilibrium trajectory radius

$$r_{eq} = r_0 \phi_0^{1/2} [(\beta Mc^2/q)r_c/(B_0 r_0^2)]^{1/4}. \quad (16)$$

If the particle enters the channel region at radius r_1 , it will stay at that radius provided $\theta_0 = 0$ and provided

$$\phi_o = (r_l/r_o)^2[(\beta Mc^2/q)r_c/(B_o r_o^2)]^{-1/2}. \quad (17)$$

The trajectory trapping constraints are found by multiplying Eq. (15) by $r dt$ and integrating. We find that at an extremum of the trajectory ($r = r_{max}$ or $r = r_{min}$),

$$\theta_o^2 = 2(I_c/L_A)[(r^2 - r_l^2)/r_c^2] + (r_o^2 v_{\phi o}^2/v_z^2)(r^2 - r_l^2), \quad (18)$$

where I_c is the channel current. Substituting $r = r_c$ or $r = r_{min}$ we find

$$\phi_o^2 = \frac{2(I_c/L_A)[1 - (r_l^2/r_o^2)] - \theta_o^2}{(r_o^2/r_c^2)[(r_c^2/r_l^2) - 1]} \quad r_l \leq r_c, \quad (19)$$

$$\phi_o^2 = \frac{2(I_c/L_A)(r_{min}^2/r_c^2)[(r_l^2/r_{min}^2) - 1] + \theta_o^2}{(r_o^2/r_{min}^2)[1 - (r_{min}^2/r_l^2)]} \quad r_{min} \leq r_l. \quad (20)$$

In the limit $r_{min} \rightarrow 0$, result (20) shows $\phi_o \rightarrow 0$. Since $r_{min} = 0$ for the channel case, this shows there is no minimum bound to ϕ_o (as there is for the wire case). Result (19) is plotted in Figs. 7-9 for the same parameter values as used in Figs. 4-6, and the equilibrium radius injection condition (17) is plotted in Fig. 7. In comparing Figs. 7-9 with Figs. 4-6 note that the minimum ϕ_o constraint is absent for the channel case. Again, however, if angular momentum is present, careful phase space tailoring of the beam will be needed to insure most of the beam will be in the acceptance region.

Useful Trapping Formulas

Simple results that give the minimal conditions for trapping a beam with a given θ_o or ϕ_o are as follows. For $\phi = 0$, $r = r_c$, and $r_l = 0$, Eq. (18) gives the familiar result

$$\theta_o = (2I_c/L_A)^{1/2} \quad (21)$$

for the trajectory with peak amplitude r_c , and angle θ_o at $r = 0$ that is trapped by the current I_c . Similarly for $\theta_o = 0$, and using $B_o = 2I_c/(cr_c)$, and setting $r_l = r_c$, we find for either the wire case or the channel case,

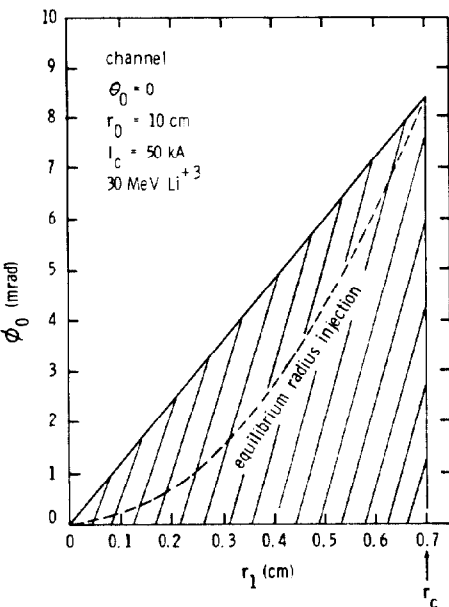


Figure 7. Channel acceptance region for $\theta_o = 0$ and $r_o = 10$ cm.

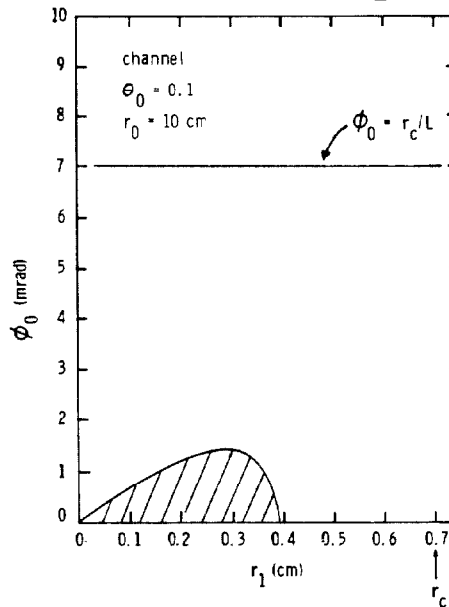


Figure 8. Channel acceptance region for $\theta_o = 0.1$ and $r_o = 10$ cm.

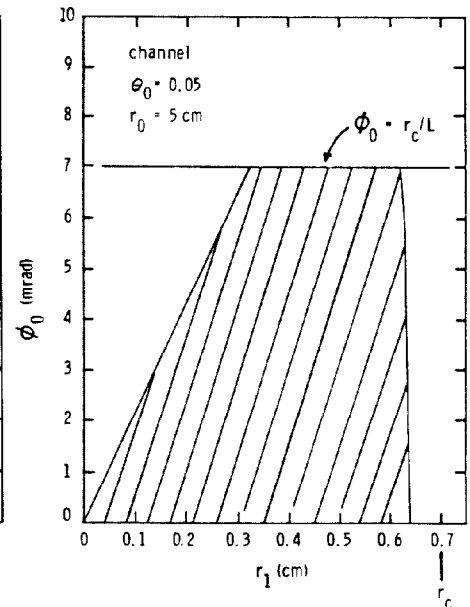


Figure 9. Channel acceptance region for $\theta_o = 0.05$ and $r_o = 5$ cm.

$$\phi_o = (r_c/r_o)(2I_c/L_A)^{1/2}. \quad (22)$$

This represents the angle ϕ_o that can be trapped due to angular momentum by a current I_c . For typical LMF parameters (30 MeV Li^{+3} , $I_c = 50$ kA, $R = 10$ cm, $r_c = 0.7$ cm) we find $\theta_o = 0.1$ and $\phi_o = 0$, or $\theta_o = 0$ and $\phi_o = 8.4$ mrad. When both θ_o and ϕ_o are non-zero, the full analysis of the previous sections must be used.

Conclusions

In real diode/transport configurations, there will be some angular momentum (i.e., $\phi_o \neq 0$) created, e.g., by combinations of diode microdivergence, beam steering errors, foil scattering, and gas scattering. Both the ballistic/lens case, and the channel case can accept $\phi_o = 0$ beams if they can be made, and can also tolerate certain amounts of $\phi_o \neq 0$. On the other hand, the wire case requires $\phi_o \neq 0$ in a carefully prepared manner.

It should be noted that there may be several constraints in addition to phase space acceptance for each transport scheme. For example, many effects such as plasma instabilities have already been examined for the channel case.^{4,5}

The above results show that in regard to angular momentum, the baseline ballistic case is the most accepting transport scheme. The channel transport scheme is less accepting. The wire transport scheme is the least accepting because it requires a tailored non-zero ϕ_o distribution to be fully accepted.

Acknowledgements

Conversations with J. T. Crow, K. R. Prestwich, R. R. Peterson, P. F. Ottinger, D. Mosher, and J. J. Watrous are gratefully acknowledged.

References

1. J. J. Ramirez et al., Proc. Eighth ANS Top. Meeting Tech. Fusion Energy, to be published.
2. C. L. Olson, Proc. 1988 Linear Accelerator Conference, CEBAF, to be published.
3. T. H. Mehlhorn et al., this conference.
4. P. F. Ottinger et al., Phys. Fluids **24**, 164 (1981).
5. D. Mosher et al., Comments Plasma Phys. and Controlled Fusion **6**, 101 (1981).